6. S. N. Frank and A. J. Bard, *ibid.,* **97,** 7427 (1975).
7. A. Ya. Gokhshtein, *Sov. Electrochem. Engl. Trans.,* **7,** 13 (1971).
8. R. E. Malpas, R. A. Fredlein, and A. J. Bard, *J. Electroanal. Chem. Interfacial Electrochem.,* **98,** 171 (1979).
9. R. E. Malpas, R. A. Fredlein, and A. J. Bard, *ibid.,* **98,** 339 (1979).
10. R. E. Malpas and A. J. Bard, *Anal. Chem.,* In press.
11. J. F. McCann and L. J. Handley, Submitted to Faraday Society Meeting (1979).
12. Y. G. Berube and P. L. DeBruyn, *J. Colloid. Interface Sci.,* **27,** 305 (1968).
13. W. H. Laflere, R. L. Van Meirhaeghe, F. Cardon, and W. P. Gomes, *Surf. Sci.,* **59,** 401 (1976).
14. H. Yoneyama, H. Sakamoto, and H. Tamura, *Electrochim. Acta,* **20,** 341 (1975).

Application of A-C Techniques to the Study of Lithium Diffusion in Tungsten Trioxide Thin Films

C. Ho,* I. D. Raistrick,* and R. A. Huggins*

Stanford University, Stanford, California 94305

ABSTRACT

The small signal a-c impedance of the cell

Li|LiAsF$_6$ (0.75M) in propylene carbonate|
    Li$_y$WO$_3$ thin film on tin oxide covered glass substrate

has been measured at room temperature as a function of frequency from 5×10^{-4} Hz to 5×10^3 Hz at various open-circuit voltages. The diffusion equations have been solved for the appropriate finite boundary conditions, and analysis of the impedance data by the complex plane method yields values for the chemical diffusion coefficient, the component diffusion coefficient, the partial ionic conductivity of lithium, and the thermodynamic enhancement factor for Li$_y$WO$_3$ as a function of y. The films of WO$_3$ were prepared by vacuum evaporation and were largely amorphous to x-rays. The chemical diffusion coefficient has a value of 2.4×10^{-12} cm^2/sec at $y = 0.1$, increasing to 2.8×10^{-11} cm^2/sec at $y = 0.26$. At short times ($t < 0.5$ sec) the interfacial charge transfer reaction is important, but at longer times the rate of lithium injection is determined by the diffusion kinetics.

Considerable interest has developed recently in the possibility of fabricating display devices based on the electrochemical injection of metal or hydrogen atoms into transition metal oxides, usually WO$_3$. The reaction may be written

$$WO_3(\text{colorless}) + yM^+ + ye^- \leftrightarrows M_yWO_3(\text{colored})$$

For each atom injected an electron enters the conduction band of the host oxide and a deep blue coloration develops. At the same time, the electronic conductivity of the oxide rapidly increases. The range of solid solubility of M in WO$_3$ may be quite extensive; typically a y value of about 0.1-0.2 is necessary for good optical contrast. The activity of M in M$_y$WO$_3$, and hence the electrode potential of the electrochromic oxide will vary continuously with y as long as a single phase solid solution is formed. If the reaction proceeds rapidly and reversibly, then the metal atoms may be repeatedly injected and removed by controlling the electrode potential of the oxide electrode with respect to a counterelectrode which acts as a source and sink of M.

Although reactions of this type have been known for several years, few data are available on basic electrochemical parameters, such as diffusion coefficients of M in the oxide or exchange current densities, even though the eventual response time of the device will be largely determined by these parameters. It is not even clear whether the rate of injection is limited by diffusion or by charge transfer at times of interest for display applications.

This paper describes a steady-state a-c technique which may be used to determine the rate-limiting process and the important kinetic parameters of an electrochromic system. It is illustrated by results obtained for the lithium-tungsten trioxide system.

Although any of several transient techniques could, in principle, be used to study this system, an a-c method was chosen since it seemed likely that, using complex plane methods, data analysis could be much simplified, especially since semi-infinite diffusion conditions cannot be assumed for the case of thin film electrodes.

Few studies of the electrochromic effect of alkali metals in WO$_3$ have been reported (1-10). Green *et al.* have studied sodium and lithium injection in WO$_3$ using both liquid and solid electrolytes (2-5, 10). The diffusion coefficient of lithium was estimated to be 2×10^{-12} cm^2/sec (3). Mohapatra (8), however, has recently reported a much higher value of 5×10^{-9} cm^2/sec. Thermodynamic data for lithium in amorphous WO$_3$ films have recently also appeared (9, 10).

Theory of the A-C Method

Alternating-current and voltage methods have, of course, been extensively used in many kinds of electrochemical systems, and several review articles are available (11-13).

In general, either current or voltage may be the controlled variable, and the phase and magnitude of the dependent variable (voltage or current, respectively) are determined with respect to this. If measurements are made over a wide-enough frequency
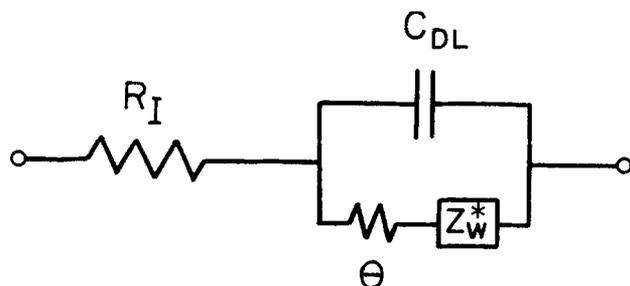
Fig. 1. The Randles equivalent circuit for the a-c response of a system with charge transfer and diffusion of the electroactive species.

range, then different physical processes may be separated through their different time constants.

The problem of the a-c response of a simple electrochemical system with either charge transfer or diffusion-limited kinetics has been considered by several authors. The equivalent circuit for this situation is due to Randles (14) and is shown in Fig. 1. This circuit will also be valid for the diffusion of a metal into an oxide electrode, if it can be assumed that diffusion is driven by a gradient in composition and not by an electric field.

In Fig. 1, R_I is the uncompensated ohmic resistance of the electrolyte and electrode, C_{DL} is the double layer capacitance of the electrode-electrolyte interface, θ is the charge transfer resistance, and Z_W^* is a complex impedance arising from the diffusion of the electroactive species.

For the case of semi-infinite diffusion

$$Z_W^* = A\omega^{-\frac{1}{2}} - jA\omega^{-\frac{1}{2}} \qquad [1]$$

where ω is the radial frequency, $j = \sqrt{-1}$, and A is a constant which contains a concentration independent diffusion coefficient. Z_W^* is often known as the Warburg impedance (15). The explicit form of A, and a more general expression for Z_W^*, which is also valid for a finite diffusion situation, are derived below.

The charge transfer resistance θ, is related to the exchange current density (I_o), through a linearization of the Butler-Volmer equation for small overpotentials (δE)

$$\theta = \frac{\delta E}{i} = \frac{RT}{nI_o\mathbf{F}} \qquad \delta E << \frac{RT}{\mathbf{F}} \qquad [2]$$

It is assumed in the derivation of this equivalent circuit that small signal conditions are met, since C_{DL}, θ and A are in general voltage or concentration dependent and lead to nonlinear behavior.

The frequency response of this circuit will be governed by the relative importance of charge transfer and diffusion in determining the current: for very slow diffusion $Z_W^* > \theta$, and for very slow charge transfer kinetics $Z_W^* < \theta$. Since Z_W^* is a function of frequency and θ is not, then an electrode reaction rate may be controlled by diffusion at low frequencies (long times) and by charge transfer at high frequencies (short times).

Derivation of Z_W^* for a thin film electrode.—The magnitude of the Warburg impedance Z_W^* is determined by the chemical diffusion coefficient of the neutral electroactive species (A) in the electronically conducting oxide electrode (B), and the explicit form of Z_W^* can be derived by solving Fick's laws with suitable initial and boundary conditions. The situation is fully analogous to the determination of chemical diffusion coefficients in solid solution electrodes by a transient galvanostatic technique discussed previously by Weppner and Huggins (16, 17).

Experimentally, the electrode is held at a constant potential E, with respect to a reference electrode of pure A, until equilibrium is reached. The composition of the sample at equilibrium is uniform and equal to A_yB. The chemical potential of A in A_yB is

$$\mu_A = \mu_A° + RT \ln \gamma_A X_A \qquad [3]$$

Here X_A is the mole fraction of A, and γ_A is its activity coefficient. If we choose $\gamma_A \to 1$ as $X_A \to 1$ then $\mu_A°$ is the chemical potential of pure A at the same temperature. Thus

$$E = -\frac{RT}{z\mathbf{F}} \ln \gamma_A X_A \qquad [4]$$

z is the charge carried by A cations, $\mathbf{F}$ and R are the gas constant and Faraday, respectively.

A small alternating voltage

$$\delta E = v_o \sin \omega t \qquad [5]$$

is now applied between the A_yB working electrode and the reference electrode, which drives the surface of the working electrode to a new time dependent concentration $X_A + \delta X_A$ (which corresponds to a stoichiometry of $A_{y+\delta y}B$). Eventually, a steady state is reached and we require an expression for the amplitude and phase of the current flowing through the cell. Since the current density depends on the gradient in concentration at the interface, through Fick's law, and the voltage depends on the chemical potential at the interface, it is necessary to either make dilute solution assumptions or else to have knowledge of the activity coefficient of A in A_yB. Since the solid solutions under consideration here are quite concentrated (X_A may be as high as 0.3) dilute solution behavior cannot be assumed and an alternative approach is adopted here which is equivalent to a knowledge of γ_A as a function of y. If we can assume that for very small changes in voltage

$$\frac{\delta E}{\delta X_A} \cong \frac{dE}{dX_A} \qquad [6]$$

We can substitute Eq. [6] into Eq. [5] and obtain

$$\delta X_A(t) = (dE/dX_A)_{X_A}^{-1} \cdot v_o \sin \omega t \qquad [7]$$

This equation describes the change in mole fraction of A at the electrode-electrolyte interface for a very small change in applied alternating voltage. $(dE/dX_A)_{X_A}$ may be obtained by differentiation of the coulometric titration curve at the appropriate composition (X_A), or as will be seen later, may, in the present case, be obtained directly from very low frequency measurements. Equation [7] represents a linearization of the dependence of concentration on voltage. The mole fraction of A at the interface is therefore a sinusoidal function of time as long as $(dE/dX_A)_{X_A}$ is constant over the range of composition δX_A.

For a diffusion experiment it is convenient to write Eq. [7] in terms of the number of atoms per unit volume (C_A), and the stoichiometry (y)

$$\delta C_A(t) = \frac{N}{V_M} \cdot \left(\frac{dE}{dy}\right)_y^{-1} \cdot v_o \sin \omega t \qquad [8]$$

Here N is Avogadro's number and V_M is the molar volume of A_yB, assumed constant over the range δy.

We therefore seek solutions of the equation

$$\frac{\partial[\delta C_A(x,t)]}{\partial t} = \tilde{D} \frac{\partial^2[\delta C_A]}{\partial x^2} \qquad [9]$$

with the initial condition of uniform concentration

$$\delta C_A(x,0) = 0 \qquad [10]$$

and the $x = l$ boundary condition given by Eq. [8]. Here l is the thickness of the oxide electrode; the coordinate system used is shown in Fig. 2. The second boundary condition is

$$\partial[\delta C_A(0,t)]/\partial x = 0 \qquad [11]$$

corresponding to an interface impermeable to A.
The diffusion coefficient used here is the chemical diffusion coefficient, which is appropriate for the diffusion of a species in an activity gradient (16). With certain assumptions, it can be related to the particle diffusion coefficient of the components (A^{z+} ions and electrons).

The solution of Eq. [9] for these conditions is given by Carslaw and Jaeger (18)

$$\delta C_A(x,t) = \alpha B \sin(\omega t + \phi) \qquad [12]$$

with

$$\alpha = \frac{N}{V_M} \cdot \left(\frac{dE}{dy}\right)^{-1} v_o \qquad [13]$$

$$B = |f| \qquad [14]$$

$$\phi = \arg(f) \qquad [15]$$

and

$$f = \frac{\cosh kx \cdot (1+j)}{\cosh kl \cdot (1+j)} \qquad [16]$$

with

$$k = (\omega/2\widetilde{D})^{1/2} \qquad [17]$$

Note that this is the steady-state solution. There is also a transient caused by starting the sinusoidal oscillation at $t = 0$. The form of this transient is given in Ref. (18).

In order to determine the current density in the system, it is necessary to evaluate $(\partial[\delta C_A]/\partial x)_{x=l}$. From Eq. [12] it may be shown that

$$\left(\frac{\partial[\delta C_A]}{\partial x}\right)_{x=l} = \tau \sin(\omega t + \beta) \qquad [18]$$

where

$$\tau = (\alpha k/\sqrt{2}d)(h^2 + s^2)^{1/2} \qquad [19]$$

and

$$\beta = \arctan\left(\frac{h+s}{h-s}\right) \qquad [20]$$

with

$$h = \sinh(2kl) \qquad [21]$$

$$s = \sin(2kl) \qquad [22]$$

$$d = \cosh^2(kl) \cdot \cos^2(kl) + \sinh^2(kl) \cdot \sin^2(kl) \qquad [23]$$
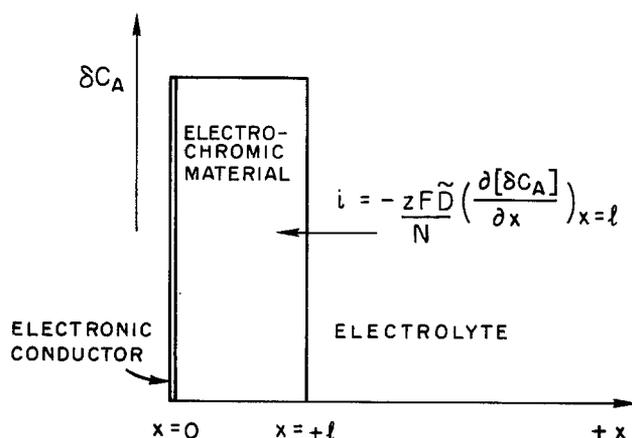
Thus, the current density

Fig. 2. The coordinate system used for the solution of the diffusion equations.

$$i_d = -\widetilde{D}\left(\frac{\partial[\delta C_A]}{\partial x}\right)_{x=l} \cdot \frac{zF}{N} \qquad [24]$$

has an amplitude

$$i_o = -\frac{zF}{2V_M}\left(\frac{dE}{dy}\right)^{-1} \cdot v_o(\omega\widetilde{D})^{1/2}\left(\frac{h^2+s^2}{d^2}\right)^{1/2} \qquad [25]$$

and a phase of β with respect to the applied voltage. Note that both the phase and the amplitude are frequency dependent.

Two extreme cases are of interest. First, consider the value of i_o for high frequencies, small $\widetilde{D}$, or thick samples, i.e., $kl >> 1$. Under these conditions $(h^2 + s^2)^{1/2}/d = 2$, and so

$$i_o = -\frac{zFV_o}{V_M}\left(\frac{dE}{dy}\right)^{-1} \cdot (\omega\widetilde{D})^{1/2} \qquad [26]$$

and

$$\beta = \arctan(1) = \pi/4 \qquad [27]$$

Thus, the phase difference between the current and the voltage is independent of frequency and is equal to 45°. Expressing this result as a complex impedance

$$Z_W^* = |Z|\cos\left(\frac{\pi}{4}\right) - j|Z|\sin\left(\frac{\pi}{4}\right)$$

$$= \frac{|Z|}{\sqrt{2}} \cdot (1-j) \qquad [28]$$

where

$$|Z| = \left|\frac{v_o}{i_o a}\right| = \left|\frac{V_M(dE/dy)}{zF\widetilde{D}^{1/2}a} \cdot \omega^{-1/2}\right| \qquad [29]$$

where a = surface area.
Comparison of Eq. [28] with Eq. [1] shows that for these conditions the preexponential factor A in the Warburg impedance has the form

$$A = \left|\frac{V_M(dE/dy)}{\sqrt{2}\,zF\widetilde{D}^{1/2}a}\right| \qquad [30]$$

The other limiting case occurs at very low frequencies, for very thin samples or for large $\widetilde{D}$
If

$$kl << 1 \qquad (i.e., \omega << 2\widetilde{D}/l^2) \qquad [31]$$

$$i_o = -\frac{zFv_o}{V_M}\left(\frac{dE}{dy}\right)^{-1} l\omega \qquad [32]$$

$$\beta = \arctan(\infty) = \frac{\pi}{2} \qquad [33]$$

Thus, under these conditions the current is 90° out of phase with the voltage and is independent of the diffusion coefficient.

Expressed as the imaginary (X) and real (R) parts of the complex impedance for these conditions

$$X = |Z|\sin\beta = |Z| = |V_M(dE/dy)/zF\omega la| = \frac{1}{\omega C_L} \qquad [34]$$

$$R = |Z|\cos\beta = |Z|\, 2k^2l^2/3a \qquad [35]$$

$$= R_L = \left|\frac{V_M}{zFa}\left(\frac{dE}{dy}\right)\left(\frac{l}{3\widetilde{D}}\right)\right| \qquad [36]$$

where C_L and R_L are the limiting low frequency capacitance and resistance. An interesting consequence of Eq. [34] and [36] is that for thin samples, it is not necessary to obtain a coulometric titration curve since simultaneous solution of these equations yields values for both the diffusion coefficient and $(dE/dy)_y$. Alternatively, if this last quantity is known independently, then the sample thickness may be calculated. Of course, no information about $(dE/dy)_y$ or l may be obtained

from the high frequency data since the diffusion is then semi-infinite in nature, and only $\tilde{D}$ may be determined.

At intermediate frequencies, when neither of the two limiting cases can be applied, the frequency response of the electrode must be analyzed using the full impedance expressions

$$Z_W{}^* = R_W - jX_W \qquad [37]$$

with

$$X_W = |Z| \sin \beta \qquad [38]$$

$$R_W = |Z| \cos \beta \qquad [39]$$

where β is given by Eq. [20], and

$$|Z_W| = |v_o/i_o a| \qquad [40]$$

where i_o is given by Eq. [25].

Complex plane representation.—Since the form of $Z_W{}^*$ is now known, the impedance of the entire circuit of Fig. 1 can be computed as a function of frequency. The most useful way of representing this result is by plotting the real (R) and imaginary (X) components of the total circuit impedance *vs.* one another in the complex plane as functions of frequency. Three such computer generated plots are shown in Fig. 3.

In Fig. 3(a), the diffusional impedance is large and a straight line of 45° slope is seen over most of the frequency range. The kinetics of the system are limited almost entirely by the rate of the diffusional process. The high frequency real axis intercept gives the value of R_I and $\tilde{D}$ may be found by analysis of the straight line portion of the curve using Eq. [28] and [29].

In Fig. 3(b) a transition is obtained such that the kinetics pass from diffusion control at low frequencies to charge transfer control at high frequencies. The semicircle at high frequencies is due to the parallel combination of C_{DL} and θ, the values of which may in principle be obtained by analysis of the high frequency data. The extrapolated real intercept of the straight line region lies at [11]

$$R_S = R_I + \theta - r \qquad [41]$$

with

$$r = 2C_{DL}A^2 \qquad [42]$$

where A is given by Eq. [30].

At very low frequencies the phase angle begins to increase due to the onset of finite length effects. This process is complete in Fig. 3(c), where R has reached its limiting value given by the sum of R_L (Eq. [36]) and ($R_I + \theta$). If the diffusion kinetics are in the proper range, there can be good separation between the charge transfer semicircle at high frequencies, the 45° line of $Z_W{}^*$ at intermediate frequencies, and the vertical line at very low frequencies, due to the finite thickness effect. $\tilde{D}$ may be obtained from either the 45° portion of the line or from R_L, determined from the limiting resistance, and Eq. [36].

Experimental Procedures

Sample preparation.—The diffusion experiments were carried out on thin films of tungsten trioxide deposited on tin oxide (700Å thick) covered glass substrates. Amorphous WO_3 films were prepared by thermal evaporation of the oxide at a rate of 30 Å/sec. The substrate temperature during evaporation was 100°C, and the pressure was maintained at 2×10^{-4} Torr of air. The method of preparation and the characterization of these films was discussed in Ref. (19), where it was also demonstrated that such films are stable in the electrolyte/solvent system used in the present experiments.
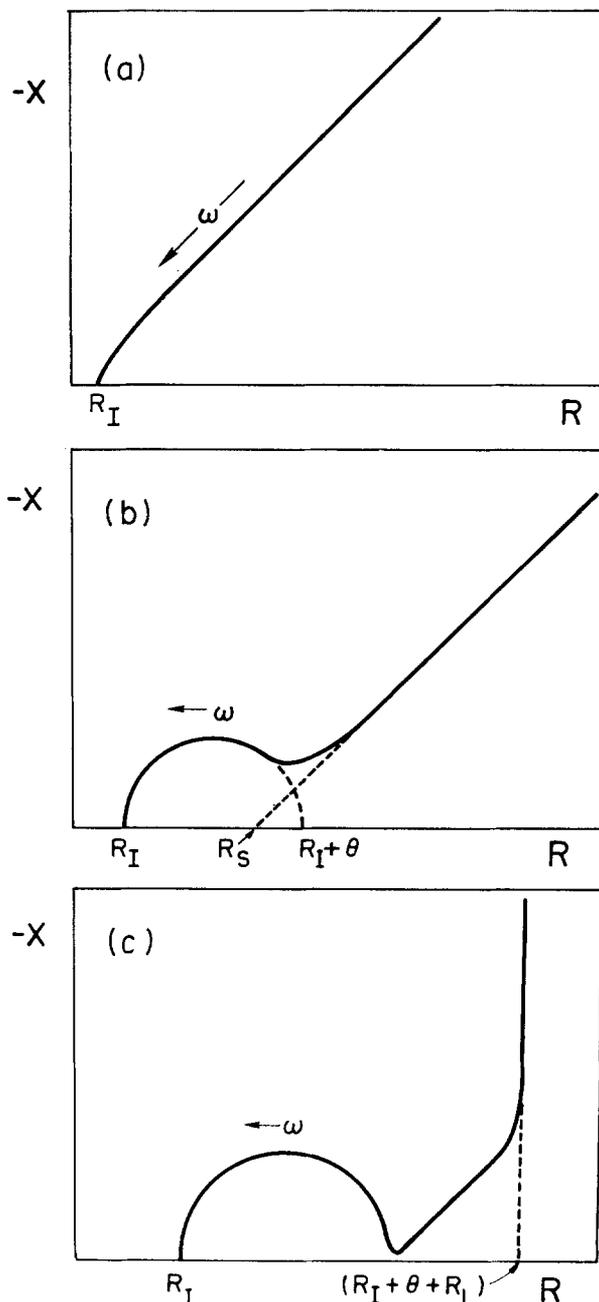

Fig. 3. Computer simulation of the complex impedance of the circuit shown in Fig. 1 for various values of the diffusion coefficient.

The results reported below were obtained on 1500Å thick films which had been heat-treated in pure oxygen for 6 hr at 350°C. This procedure was adopted in order to dry the films and to ensure that the stoichiometry was in fact WO_3. X-ray diffraction experiments indicated that the initially amorphous films, which showed only a broad diffuse scattering centered on a d value of 3.6Å, developed some crystallinity on undergoing this heat-treatment. Several sharp reflections developed, which could be indexed on the same unit cell as the high temperature tetragonal modification of WO_3 (in agreement with the observations of Green [10], but with slightly reduced lattice parameters). The sharp reflections were superimposed on a diffuse background similar to that of the unheated, treated films.

A density of 5.2 g/cm³ was used in the calculation of the results below, based on a comparison of the measured film volume (using interferometry) and chemical analysis (19).

Electrochemical measurements.—Measurements were made using a three electrode configuration. Both

counter and reference electrodes were pure lithium metal, and the electrolyte was 0.75M LiAsF₆ in propylene carbonate. The electrolyte was dried by prolonged agitation with lithium chips. All materials and the electrochemical cell were kept in a helium-filled dry box. Measurements were made at 300°K.

The thin film working electrode was held at constant voltage (and hence composition) by a Princeton Applied Research Model 173 potentiostat. A small alternating signal from a Hewlett Packard HP3110B oscillator was then superimposed on the constant voltage and the current flowing in the counter-working electrode circuit was monitored via a standard resistance. The circuit is shown in Fig. 4. The amplitude of the signal applied to the sample was always less than 10 mV and the frequency range covered extended from 5×10^{-4} Hz up to 5 kHz.

Above 20 Hz, the amplitude and phase of the current with respect to the applied voltage were measured directly using a PAR Model 5204 two-phase lock-in analyzer. Above about 100 Hz, small corrections were made to compensate for the attenuation and phase shift introduced into the signal by the potentiostat. This was achieved by comparing the a-c perturbation of the potential difference between the reference and working electrodes directly with the output of the oscillator.

Below 20 Hz, the signals corresponding to current and voltage were amplified using a PAR Model 113 preamplifier and fed to the analog-to-digital converters of a Digital Equipment Corporation Lab 8e computer, where the two signals were averaged over several cycles and compared.

Results

The change in open-circuit voltage (E) with composition (y) is plotted in Fig. 5. The order in which the points were taken is indicated, showing that the measurements were in fact made at equilibrium. Results of the two other thermodynamic studies are also shown for comparison (9, 10).

The complex impedance data are summarized in Fig. 6 and 7. In Fig. 6, the higher frequency data are shown for four open-circuit voltages. At the highest voltage (2.6V with respect to pure lithium), a straight line of slope 45° was obtained from about 0.01 Hz up to 5 kHz, corresponding to complete diffusion control of the electrochemical insertion reaction over the whole of the available frequency range. At lower open-circuit voltages (corresponding to higher lithium concentrations in the film), the separation of a semicircular region is evident at higher frequencies and, at the same time at lower frequencies, the 45° line begins to give way to a vertical line under the influence of finite length effects. The 5 Hz points are marked on the plots, and it can be seen that at this frequency a gradual transition from diffusion-controlled to charge transfer-controlled kinetics takes place as lithium is added to the film.

Complex impedance data for the lowest frequencies are shown in Fig. 7. In this frequency range, the rate
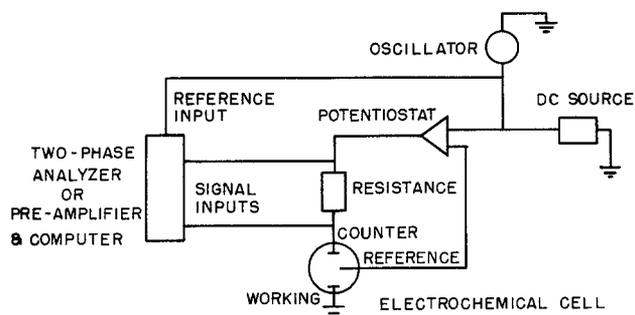
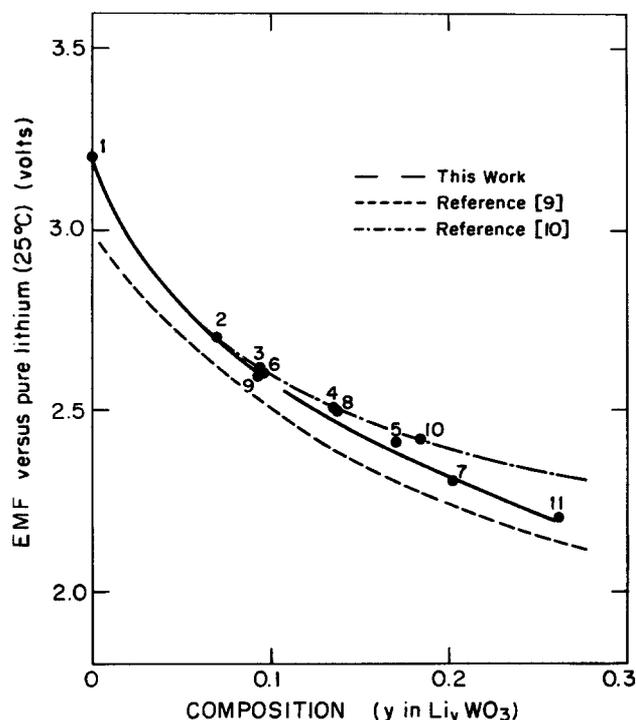**Fig. 5.** Coulometric titration curve for Li$_y$WO₃. The numbers indicate the order in which the data were taken. Results of Mohapatra and Wagner (9) and Green (10) are shown for comparison.
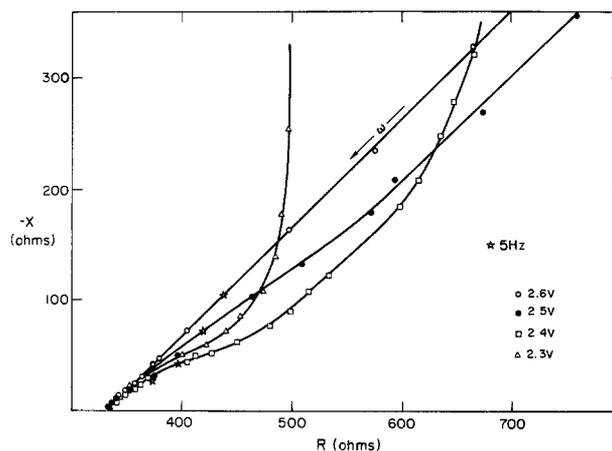
Fig. 6. High frequency complex impedance data

of lithium injection is always diffusion-controlled. The onset of finite length effects shifts to higher frequencies and the low frequency limiting resistance decreases as more lithium is added to the film, indicating that the diffusion coefficient is steadily increasing. Values of the chemical diffusion coefficient, $\tilde{D}$, were obtained from either the 45° straight line region or else from the low frequency limiting behavior. At high voltages, in the semi-infinite diffusion regime, data analysis presented no problems. Both the real and the imaginary parts of the impedance are proportional to $\omega^{-1/2}$. This is illustrated in Fig. 8 for the highest voltage case. $\tilde{D}$ was calculated from such plots using Eq. [28] and [29]. Alternatively, $\tilde{D}$ can be calculated from the low frequency limiting resistance (Eq. [36]). The low frequency limiting capacitance (obtained from Eq. [34]) yields values of $(dE/dy)_y$ which were used in the computation of $\tilde{D}$. Relevant data are given in Table I.
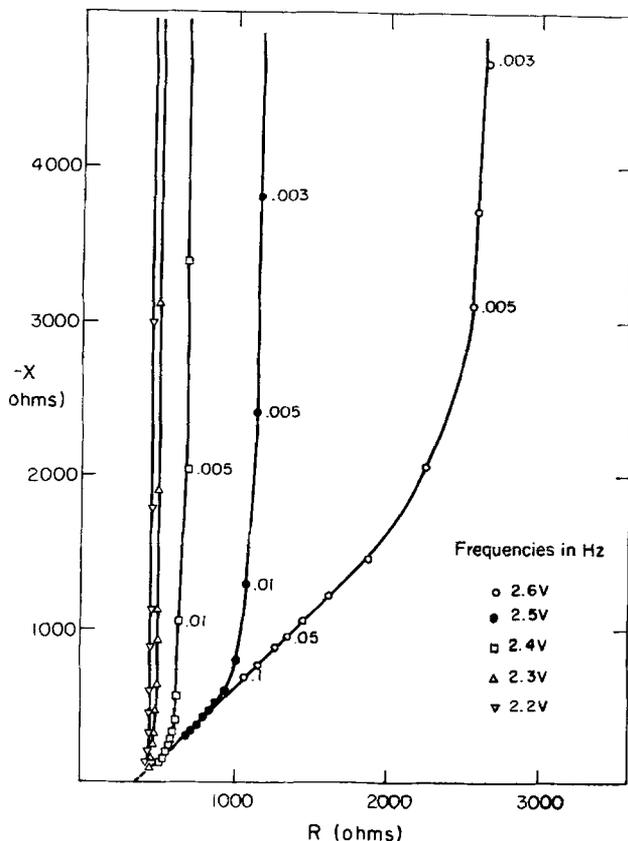
Fig. 7. Low frequency complex impedance data

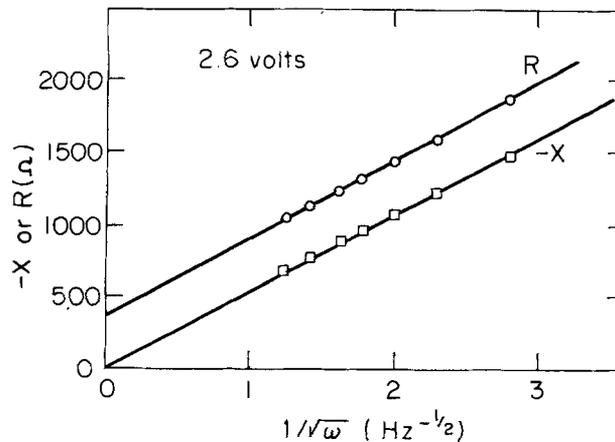Fig. 8. Real and imaginary parts of the complex impedance plotted vs. $\omega^{-1/2}$.

Use of R_L for the calculation of $\tilde{D}$, however, has a disadvantage in the particular case of the data under consideration here. R_L is measured from the point at which the 45° straight line would intercept the real axis (see Fig. 3b), and thus, if this point is not well-defined, due to overlap of the diffusion- and charge transfer-controlled regions, an inaccuracy is introduced into the calculation of $\tilde{D}$. The overlap also prevents accurate evaluation of C_{DL} and θ.

These difficulties could, in principle, be overcome by fitting the low frequency impedance data to the full impedance expression (Eq. [38] and [39]). However, the complicated nature of these functions makes this a difficult task which was not attempted here.

Values of the diffusion coefficients calculated for lower voltages (2.2 and 2.3V) are, therefore, of lower accuracy than those for higher voltages.

Discussion

The a-c method.—The technique described in this paper shows itself to be a useful tool for the study of diffusion in thin film solid electrodes, although it is by no means limited in application to such systems. The method appears to have a number of advantages over alternative, transient techniques (such as voltage

or current step experiments), the most important being that more information is obtained through relatively simple data analysis procedures using the complex impedance plane method. Even in situations where there is extensive overlap of the charge transfer- and diffusion-controlled regions, or where the diffusion coefficient is sufficiently high to introduce finite length effects, much important information can be obtained by inspection of the complex impedance plot. The same information is, of course, also contained in the transient response of linear systems, but data acquisition (particularly at short times) and integral transform analysis so complicate the procedure that often only data obtained over a limited time period (for example, when the change in dependent variable is proportional to $\sqrt{t}$) are actually useful. As may be seen from the present results, the region in which the impedance is proportional to $\omega^{1/2}$ (or in which E would be proportional to $t^{1/2}$ in a current step experiment) may be very limited or nonexistent. Under these circumstances, the complex impedance method at the very least gives an indication of the experimentally important phenomena contributing to the time response of the system. Often a useful limiting region can be identified (for example, the very low frequency response for thin films) which can be used to extract numerical values for kinetic parameters.

A further advantage of using a steady-state method is that the response signal can be critically evaluated at each frequency, and further averaging (at low frequencies) or filtering (at high frequencies) can be employed.

Like the galvanostatic intermittent titration technique described by Weppner and Huggins (16), the a-c method is capable of very high resolution with respect to composition and is therefore applicable to phases with rather narrow ranges of stoichiometry.

The application of this method is, of course, dependent on the validity of a number of assumptions.

Table I. Thermodynamic and kinetic data

Composition* (y in L_yWO_3)	Open circuit voltage (vs. Li)	$\tilde{D}$ (cm² sec⁻¹)	$\left(\dfrac{dE}{dy}\right)_y$**	$\dfrac{d \ln a_{Li}}{d \ln C_{Li}}$	D_k (cm² sec⁻¹)	σ_{Li} (Ω^{-1} cm⁻¹)
0.097	2.60	2.4×10^{-12}†	5.0	18.9	1.3×10^{-13}	1.04×10^{-9}
0.138	2.50	4.9×10^{-12}†	3.6	19.4	2.5×10^{-13}	3.0×10^{-9}
0.170	2.40	1.5×10^{-11}††	4.0	26.5	5.7×10^{-13}	8.1×10^{-9}
0.201	2.30	2.6×10^{-11}††	3.8	29.8	8.7×10^{-13}	1.5×10^{-8}
0.260	2.20	2.8×10^{-11}††	3.6	36.5	7.7×10^{-13}	1.7×10^{-8}

* Calculated assuming a density of 5.2 g cm⁻³.
** Calculated from Eq. [34].

† $\tilde{D}$ calculated from Eq. [29].

†† $\tilde{D}$ calculated from Eq. [36].

The first of these is that the boundary conditions used in the solution of Fick's diffusion equation are correct. The greatest difficulty will usually lie in the assumption that the potential of the cell is a measure of the lithium activity at the interface between the electrolyte and the electrode. This is only true if the electrode is a predominantly electronic conductor. In the present case, there seems to be good evidence that this is so. The high electronic conductivity of tungsten bronze phases is well-established (20); values are much higher than ionic conductivities calculated from previous or present measurements of diffusion coefficients, although direct measurements of partial ionic conductivities have not been made.

A second assumption implicit in the derivation given above is that the driving force for diffusion is only a gradient in composition, and that the electric field in the electrode is negligible. This, of course, will be true in view of the high electronic conductivity mentioned above.

Thirdly, in order for the solution of the diffusion equations to be correct, it must be assumed that the system is linear. In other words, the diffusion coefficient is assumed to be independent of concentration over the range of alternating voltage applied. In practice, the applied voltage can be made very small, so that the measured impedance becomes independent of amplitude. This test is very easy to carry out due to the steady-state nature of the experiment. It seems likely that the diffusion coefficient will change rather slowly with composition, and hence voltage, except in very narrow phases where rapid variation of the thermodynamic enhancement factor may be expected (16). Similar considerations of linearity also apply of course at higher frequencies where the double layer capacitance and charge transfer resistance might also show voltage dependent behavior.

Kinetic properties of WO₃ thin film electrochromic electrodes.—The primary observation concerning the kinetics of lithium incorporation into WO₃ thin films is that both diffusion and interface kinetics are important. At long times (low frequencies), the interface is essentially at equilibrium, and diffusion of neutral lithium in a concentration gradient limits the rate of coloration of the oxide. At times shorter than about 0.5 sec however, charge transfer kinetics limit the rate of injection. The following considerations are relevant.

(i) Firstly, the thermodynamic and kinetic properties of WO₃ thin films are very dependent on the method of preparation (6), and in particular are dependent on the degree of crystallinity of the films. The results given here, although typical of films which show relatively rapid coloration on lithium injection, must not be regarded as applying to all WO₃ films. A detailed study of the thermodynamics and kinetics of different kinds of films is currently underway and the results will be published separately.

(ii) Secondly, the experiments reported here are small signal experiments. In a practical device much larger voltages or currents will be applied to the samples with several consequences. First, the reaction resistance θ will change with applied voltage due to both the change in lithium concentration at the interface and the inherent voltage dependence of the heterogeneous charge transfer reaction. Secondly, large voltage differences across the interface will have important effects on the rate of bleaching as discussed by Faughnan *et al.* (21). If the potential of the surface layer of WO₃ is increased beyond about 3V with respect to lithium, then the surface will become depleted of lithium and, since the electronic conductivity falls as lithium is removed, an electric field will develop in the electrochromic which will tend to increase the rate of lithium removal. This might happen, for example, when the WO₃ is bleached under constant current conditions, when the diffusion process

cannot indefinitely support the current. A third effect of higher voltages will occur under rapid coloration conditions where the voltage falls to such low values that a concentration driven phase change on the surface of the oxide might be irreversible. Mohapatra and Wagner (9), for example, found that the chemical potential of lithium in amorphous Li$_y$WO₃ was constant for $y > 0.4$ (approximately 2V *vs.* Li). If this constant activity corresponds to a two- or three-phase region, then the new phase(s) formed may have very slow or irreversible kinetics.

In summary, therefore, small signal results should not be taken as a definitive measure of how an electrochromic device would operate under large signal conditions.

The charge transfer resistance of the interface was found to be 100-150 Ω/cm². As discussed in the Results section, an overlap of the diffusion response and the charge transfer response prevents an accurate evaluation of this resistance and its voltage dependence. The corresponding exchange current density is 8×10^{-5}-1.3×10^{-4} A/cm², a value which will depend on the concentration of Li$^+$ in the liquid electrolyte as well as electrode material parameters. Mohapatra (8) has suggested a value as high as 2×10^{-3} A/cm² for lithium injection. Somewhat smaller values (5×10^{-6}-3×10^{-5} A/cm²) have been found by Crandall and Faughnan (22) for the injection of hydrogen into amorphous WO₃.

Chemical diffusion coefficients for low lithium concentrations are in good agreement with the value of 2×10^{-12} cm²/sec suggested by Green (3). An increase with increasing lithium concentration of about one order of magnitude is observed, but the values are still much lower than the 5×10^{-9} cm²/sec reported by Mohapatra (8). The thermodynamic results given by Mohapatra and Wagner in Ref. (9), however, were in very good agreement with the results of the present study. More recent results by Green (10) show a slightly smaller value for $\widetilde{D}$ of 4×10^{-13} cm²/sec on films which also have similar coulometric titration curves. Green also suggested that rapid diffusion along grain boundaries is followed by much slower diffusion into the bulk of the grains, with an associated diffusion coefficient of about 6×10^{-16} cm²/sec. In the present study, no evidence for two diffusion processes, either in series or in parallel has been found, as the form of the results is adequately explained by a single diffusion coefficient.

As discussed by Weppner and Huggins (16), the chemical diffusion coefficient $\widetilde{D}$ is related to the component diffusion coefficient D_k by the relation

$$\widetilde{D} = D_k \frac{d \ln a_{Li}}{d \ln C_{Li}} \qquad [43]$$

for the case where the electronic transference number is close to unity. In this equation the activity and concentration terms refer to neutral lithium. Hence

$$\widetilde{D} = - D_k \frac{dE}{dy} \frac{zF}{RT} y \qquad [44]$$

and since

$$D_k = kTb \qquad [45]$$

and

$$\sigma_{Li} = z^2 F^2 C_{Li} b \qquad [46]$$

where b is the general mobility and σ the partial conductivity of Li$^+$ ions

$$\sigma_{Li} = \frac{zF\widetilde{D}}{V_M} \left(\frac{dE}{dy} \right)^{-1} \qquad [47]$$

Numerical values for D_k and σ_{Li} are given in the table. Like the chemical diffusion coefficient, these quantities appear to increase with increasing lithium con-

tent, the most rapid rate of increase occurring around $y = 0.17$.

In summary, a general steady-state a-c method has been described which allows the diffusion coefficient of a species in an electronically conducting thin film electrode to be determined. In addition, qualitative information about the kinetics of the interface charge transfer reaction has been obtained, and it is believed that in some situations detailed interfacial kinetic data could be obtained. The method has a number of advantages over transient current or voltage step techniques, stemming partly from the method of analysis in the frequency domain which allows a clear distinction to be drawn between interface and bulk processes.

Acknowledgment

REFERENCES

1. H. N. Hersh, W. E. Kramer, and J. H. McGee, *Appl. Phys. Lett.,* **27**, 646 (1975).
2. R. J. Colton, A. M. Guzman, and J. Wayne Rabalais, *J. Appl. Phys.,* **49**, 409 (1978).
3. M. Green, W. C. Smith, and J. A. Weiner, *Thin Solid Films,* **38**, 89 (1976).
4. M. Green and K. S. Kang, *ibid.,* **44**, L19 (1977).
5. W. C. Dautremont Smith, M. Green, and K. S. Kang, *Electrochim. Acta,* **22**, 751 (1977).
6. H. R. Zeller and H. U. Beyeler, *J. Appl. Phys.,* **13**, 231 (1977).
7. T. J. Knowles, *Appl. Phys. Lett.,* **31**, 817 (1978).
8. S. K. Mohapatra, *This Journal,* **125**, 284 (1978).
9. S. K. Mohapatra and S. Wagner, *ibid.,* **125**, 1603 (1978).
10. M. Green, *Thin Solid Films,* **50**, 145 (1978).
11. M. Sluyters-Rehbach and J. H. Sluyters, in "Electroanalytical Chemistry," Vol. 4, A. J. Bard, Editor, pp. 1-128, Marcel Dekker, New York (1970).
12. D. D. Macdonald, "Transient Techniques in Electrochemistry," p. 229, Plenum Press, New York (1977).
13. D. E. Smith, in "Electroanalytical Chemistry," Vol. 1, A. J. Bard, Editor, pp. 1-155, Marcel Dekker, New York (1966).
14. J. E. B. Randles, *Discuss. Faraday Soc.,* **1**, 11 (1947).
15. E. Warburg, *Ann. Physik,* **67**, 493 (1899); **6**, 125 (1901).
16. W. Weppner and R. A. Huggins, *This Journal,* **124**, 1569 (1977).
17. W. Weppner and R. A. Huggins, *Annual Review of Materials Science,* R. A. Huggins, Editor, p. 269, Annual Reviews Inc., Palo Alto (1978).
18. H. S. Carslaw and J. C. Jaeger. "Conduction of Heat in Solids," 2nd Ed., p. 105, Oxford Univ. Press, Oxford (1959).
19. J. P. Randin, *J. Electron. Mater.,* **7**, 47 (1978).
20. P. J. Wiseman and P. G. Dickens, in "MTP International Review of Science." Inorganic Chemistry. Series II. Vol. 10, L. E. J. Roberts, Editor, p. 211, London (1975).
21. B. W. Faughnan. R. S. Crandall. and M. A. Lampert, *Appl. Phys. Lett.,* **27**, 275 (1975).
22. R. S. Crandall and B. W. Faughnan, *Appl. Phys. Lett.,* **28**, 95 (1976).

Development of Sulfur-Tolerant Components for the Molten Carbonate Fuel Cell

A. F. Sammells,* S. B. Nicholson, and P. G. P. Ang*

Institute of Gas Technology, Chicago, Illinois 60616

ABSTRACT

The sulfur tolerance of candidate anode and anode current collector materials for the molten carbonate fuel cell were evaluated in an electrochemical half-cell using both steady-state and transient potentiostatic techniques. Hydrogen sulfide was introduced into the fuel at concentrations of 50 and 1000 ppm. At the higher sulfur concentration using low BTU fuel, both nickel and cobalt were observed to undergo a negative shift in their open-circuit potentials, and high anodic and cathodic currents were observed compared with clean fuels. Exchange currents measured using the transient potentiostatic technique were not greatly affected by 50 ppm H_2S introduced into the fuel. However, at higher sulfur concentrations, higher apparent exchange currents were observed, indicating a probable sulfidation reaction. Of the new anode materials evaluated, $Mg_{0.05}La_{0.95}CrO_3$ and TiC showed good stability in the anodic region. With the former material, exchange current densities in low BTU fuel were calculated to be $\simeq 8$ mA/cm^2 at 650°C, lower values than found for either nickel or cobalt anodes under similar conditions. Of the anode current collector materials evaluated, high stabilities were found for 410 and 310 stainless steels. The implications and relevance of these results on fuel cell performance are discussed.

The essential components which comprise the molten carbonate fuel cell are a porous nickel or cobalt anode, and a porous nickel oxide cathode, which are separated by an ionically conducting molten carbonate mixture supported on a lithium aluminate matrix. These components together are commonly referred to as the tile. To date, these fuel cell components have shown good electrochemical performance and corrosion stability under cell operating conditions over several thousand hours in the absence of sulfur-containing species in the fuel and oxidant. However, commercialization of this